Available online at www.sciencedirect.com
ScienceDirect
Journal of Organometallic Chemistry 692 (2007) 1511–1518
Journal of Organometallic Chemistry
www.elsevier.com/locate/jorganchem

Electronic states of radical cations of all-*trans* oligo[methyl(phenyl)silane]

Hiroto Tachikawa [a,*], Hiroshi Kawabata [b]

[a] *Division of Materials Chemistry, Graduate School of Engineering, Hokkaido University, Sapporo 060-8628, Japan*
[b] *Venture Business Laboratory, Kyoto University, Kyoto 606-8501, Japan*

Received 1 November 2006; received in revised form 28 November 2006; accepted 29 November 2006
Available online 14 December 2006

Abstract

The electronic states of radical cations of oligo[methyl(phenyl)silane] ($OMPSi^+$) with all *trans* form ($n = 2$–8, where n is number of monomer unit of OMPSi) have been investigated by means of density functional theory (DFT) calculation to shed light on the mechanism of hole-transport in oligosilanes with phenyl group in the side chain. For the shorter oligomers ($n < 3$), the hole (unpaired electron) was widely distributed equivalently in both the Si main and side chains (55% for the Si main chain and 45% for the side chain). The distribution of hole on the chains was largely changed as a function of chain lengths (n). Ratios of the hole distribution on the main and side chains became almost constant at $n = 7$–8: 70% of spin density was distributed on the Si-main chain and 30% on the side-chain, which is much different from that of oligo(dimethyl)silane (the spin density on the methyl side chain was less than 3% of spin density). From these results, it was concluded that the hole in $OMPSi^+$ can transfer by the mechanism for both intermolecular and the intrachain hole-transfer processes.

Keywords: Oligosilane; Radical cation; DFT; Ab initio; Spin density; Excitation energy

1. Introduction

Recently, polysilanes have been extensively utilized as hole and electron transport materials in organic multilayer light emitting diodes (LEDs), one-dimensional semi-conductors, photo-resist materials, and high-density optical data storage materials [1–10]. These characteristic features are originated from high hole mobility of 10^{-4} cm^2 V^{-1} s^{-1} and a low-lying excited state of polysilanes at doped state. Therefore, determination of the electronic structures for ionic states at both ground and excited states is an important theme in development of new materials of silane systems.

Charge transport in charge-injected polysilane has been investigated extensively using time-of-flight [11,12] and time resolved microwave conductivity techniques [13–17]. These experiments indicate that thermal activation and field-assistance enhance the hole mobility in polysilanes.

To elucidate mechanism of hole and excess electron transfers in polysilanes, several experiments have been carried out. In particular, the effects of substitution of side-group on the charge conductivity of oligo- and polysilanes have been investigated from experimental points of view. Seki et al. have recently measured [16] the transient absorption spectra of radical cations of a variety of substituted polysilanes by means of pulse radiolysis technique. They suggested that phenyl ring bonded to the Si–Si skeleton plays an important role in hole transport process. If the side chain is only composed of alkyl groups, the hole mobility is significantly slower than that of the phenyl group. As a reason for the high hole mobility in the polysilane with phenyl groups in side-chain, two reasons have been considered as follows: (1) σ–σ conjugation along the Si–Si backbone is more favorite in the polysilane with phenyl ring than that with alkyl group because the

* Corresponding author. Fax: +81 11 706 7897.
E-mail address: hiroto@eng.hokudai.ac.jp (H. Tachikawa).

0022-328X/$ - see front matter © 2006 Elsevier B.V. All rights reserved.
doi:10.1016/j.jorganchem.2006.11.053

structural conformation of the former polymer is well aligned by steric effect. The other reason is (2) the electronic states of polysilane are changed by the substitution of phenyl group in the side-chain. However, details of the hole transport mechanism is still not clearly understood.

From theoretical points of view, several ab initio and density functional theory (DFT) calculations have been carried out to elucidate the structures and electronic states of radical ions of oligo- and polysilanes. Recently, Toman et al. [18] performed a conclusive investigation for ion radicals of oligo[methyl(phenyl)silane] (OMPSi). They assigned explicitly infrared (IR) band of $MPSO^{+} \rightarrow OMPSi^{+}$ using DFT calculation. In previous papers, we investigated theoretically the electron transfer process in radical cation of oligo(dimethyl)silane [19] at the ground and excited states. The intermolecular electron transfer between oligomer chains does not occurred at the ground state, whereas it takes place at the excited states.

In the present study, density functional theory (DFT) calculations were applied to the neutral and radical cations of OMPSi to elucidate the mechanism of hole transport in oligosilane radical cations with the phenyl group. As be known, the first excitation band plays an important role in electron conductivity of semi-conductor. Hence, the excitation energies are calculated as a function of chain length (n). For comparison, the electronic states of oligo(dimethyl)silane (ODMSi) were investigated with the same matter.

2. Method of calculations

The geometries of neutral, radical cations and dications of OMPSi ($n = 2$–8) with all *trans* form were fully optimized at the DFT(B3LYP)/3-21G(d) level of theory. The end-groups were capped by the hydrogen atoms. We assumed syndiotactic structure throughout for the oligomers. All *trans* forms were only treated for the initial structures throughout in the present study. The spin densities and hyperfine coupling constants were calculated at the B3LYP/6-311+G(d) level. Using the optimized geometries, the excitation energies were calculated by means of time-dependent (TD)-DFT method. Six excited states were solved in the TD-DFT calculations. All hybrid DFT and ab initio calculations were carried out using Gaussian03 program package [20]. Note that the similar levels of theory give reasonable features for several molecular device systems [21–23].

3. Results

3.1. Structures of neutral and radical cation of OMPSi

First, the geometrical structures of neutral OMPSi with all-*trans* form ($n = 2$–8) are fully optimized at the B3LYP/3-21G(d) level. Definition of geometrical parameters is given in Fig. 1, and the selected optimized parameters for $n = 2$–8 are listed in Tables 1 and 2. The bond lengths of Si–Si atoms of neutral OMPSi are distributed in the range 2.34–2.37 Å. When OMPSi is ionized, the bond lengths are slightly elongated because the electron is removed from the Si–Si bonding orbital of OMPSi. For example, the bond length of Si(1–2) for $n = 8$ is changed from 2.3583 to 2.3786 Å by the ionization. This change is larger in shorter oligosilanes.

The dihedral angles of OMPSi are also changed by the ionization of OMPSi. The angles are distributed in the range 145–180°, indicating that the oligomers have transoid forms. Four dihedral angles of neutral OMPSi for $n = 7$ are calculated to 154.0°, 156.1°, 144.5°, and 157.9°, whereas those of $OMPSi^{+}$ are be 156.6°, 156.6°, 154.9° and 155.8°.

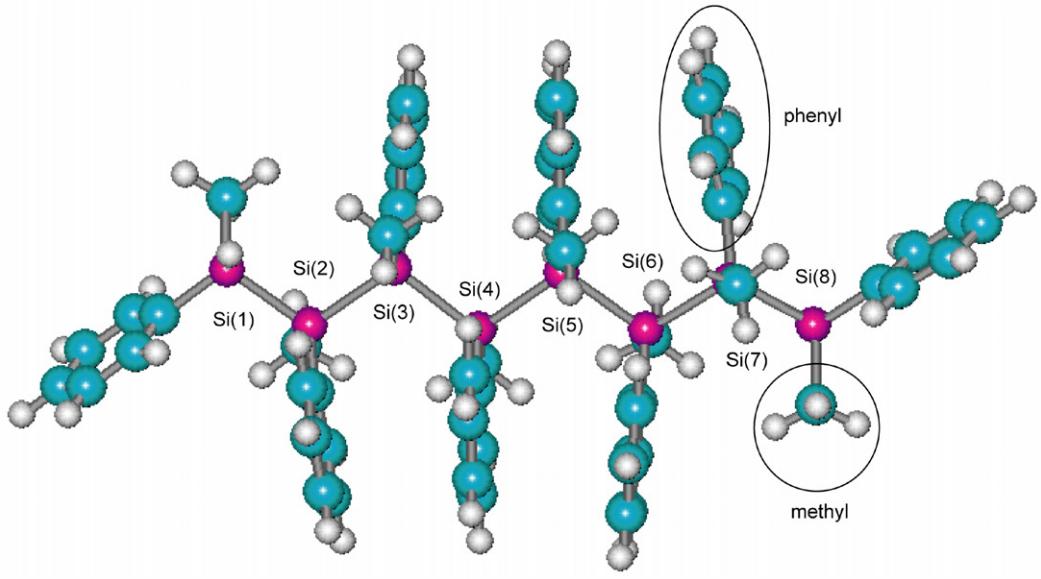

Fig. 1. Schematic illustration of structure of oligo[methyl(phenyl)silane] (OMPSi, $n = 8$).

Table 1
Optimized geometrical parameters of Si–Si bond lengths (in Å) of neutral and cation radicals of oligo[methyl(phenyl)silane]s (OMPSi and $OMPSi^+$) calculated at the B3LYP/3-21G(d)

State	n	Si(n) to Si($n+1$) length (Å)						
		Si(1–2)	Si(2–3)	Si(3–4)	Si(4–5)	Si(5–6)	Si(6–7)	Si(7–8)
Neutral	3	2.3505	2.3446					
	4	2.3540	2.3511	2.3540				
	5	2.3493	2.3559	2.3573	2.3603			
	6	2.3504	2.3576	2.3618	2.3642	2.3584		
	7	2.3510	2.3597	2.3635	2.3717	2.3599	2.3581	
	8	2.3583	2.3627	2.3728	2.3614	2.3645	2.3565	2.3568
Cation	3	2.4339	2.4244					
	4	2.4109	2.3996	2.4121				
	5	2.3956	2.3941	2.3965	2.3984			
	6	2.3838	2.3919	2.3979	2.3930	2.3880		
	7	2.3778	2.3860	2.3931	2.3966	2.3892	2.3808	
	8	2.3786	2.3833	2.3889	2.4003	2.3867	2.3828	2.3747

Table 2
Optimized geometrical parameters (Si–Si–Si–Si dihedral angle in degrees) of neutral and cation radicals of oligo[methyl(phenyl)silane]s (OMPSi and $OMPSi^+$) calculated at the B3LYP/3-21G(d)

State	n	Dihedral angle (°)				
		Si(1–2–3–4)	Si(2–3–4–5)	Si(3–4–5–6)	Si(4–5–6–7)	Si(5–6–7–8)
Neutral	4	180.0				
	5	154.8	156.6			
	6	154.7	174.1	150.6		
	7	154.0	156.1	144.5	157.9	
	8	159.1	145.1	160.9	151.7	176.3
Cation	4	161.6				
	5	159.6	159.8			
	6	156.0	156.7	156.3		
	7	156.6	156.6	154.9	155.8	
	8	155.3	157.2	158.4	175.8	164.7

For comparison, the similar calculations are carried out for oligo(dimethyl)silane (ODMSi). In the case of radical cation of oligo(dimethyl)silane ($ODMSi^+$) for $n = 7$, these angles are 159.4°, 171.1°, 171.1° and 159.4°, meaning that Si skeleton of $ODMSi^+$ is close to the regular all *trans* form. The result indicates that the Si–Si skeleton in $OMPSi^+$ is more deformed than that of $ODMSi^+$. From these results, it is concluded that the σ–σ conjugation along the Si–Si backbone is not enhanced by the phenyl-substitution. Instead, the σ–σ conjugation in the polymer with methyl group is more favorite than that of phenyl group.

To check the stabilities of the optimized structures, the vibrational frequencies are calculated for OMPSi and $OMPSi^+$ with $n = 1$–2. All vibrational frequencies calculated are positive, indicating that the structures are located at the local minima on the ground state potential energy surface.

3.2. Spin densities of $OMPSi^+$

Spin densities on the Si main and side chains of $OMPSi^+$ ($n = 2$–8) are plotted in Fig. 2a as a function of chain length (n). We discuss the electronic states of $OMPSi^+$ using the results obtained by the B3LYP/6-311+G(d,p)//B3LYP/3-21G(d) level. In the shortest oligomer ($n = 2$), the spin densities on the main and side chains are calculated to be 0.56 and 0.44, respectively, indicating that the unpaired electron on the main chain is slightly larger than that of the side chain. This difference becomes wider in longer chains, and it reaches a limiting value around $n = 8$. In the case of $n = 8$, the spin densities on the main and side chains are 0.71 and 0.29, respectively. From these results, it is concluded that the hole is distributed on both main and side chains. About 30% of hole is distributed on the side chain.

For comparison, the similar calculation is carried out for the oligo(dimethyl)silane ($ODMSi^+$). The spin densities on the Si main and methyl side chains are plotted in Fig. 2a as a function of n. As clearly shown, the hole is fully localized on the Si main chain in the case of $ODMSi^+$. For example, the spin densities on the main and side chains for $n = 7$ are 0.92 and 0.08, respectively, indicating that almost all spin densities are localized on the Si main chain. The feature is much different from that of $OMPSi^+$. This difference causes the difference of the mechanism of hole transports in both $OMPSi^+$ and $ODMSi^+$ Scheme 1.

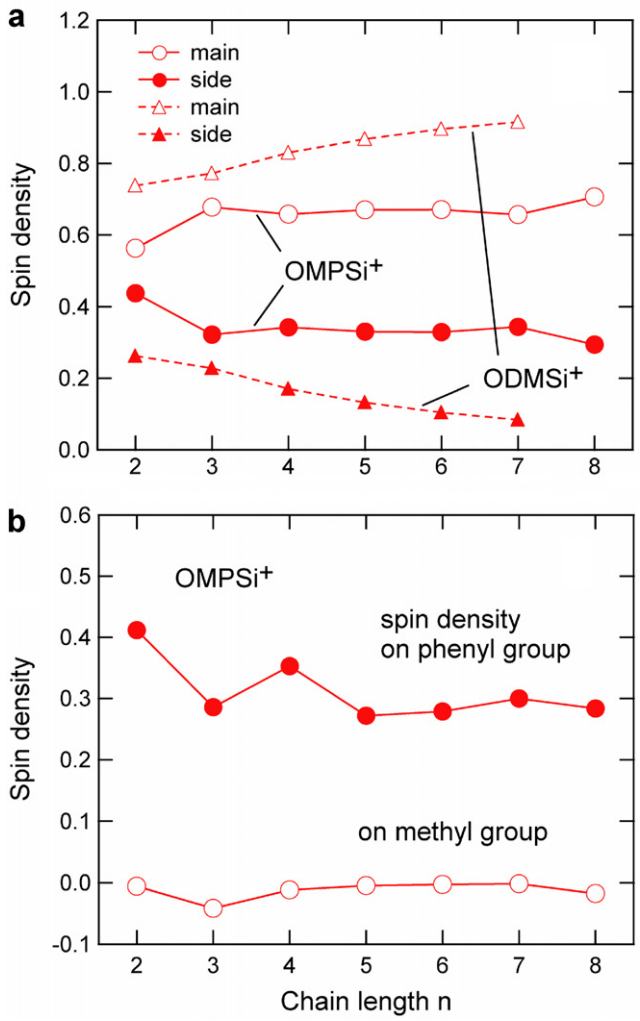

Fig. 2. Spin densities on (a) Si main and side chains of $OMPSi^+$ plotted as a function of chain length (n). The calculation is carried out at the B3LYP/6-311+G(d)//B3LYP/3-21G(d) level. Solid and dashed lines indicate spin densities of $OMPSi^+$ and $ODMSi^+$, respectively. (b) Spin densities on phenyl and methyl groups of $OMPSi^+$.

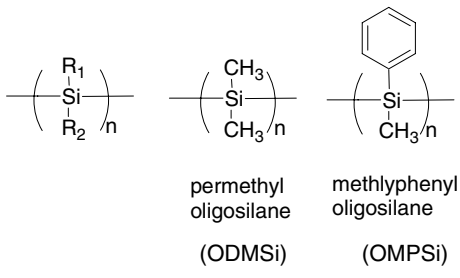

Scheme 1.

The side chain of $OMPSi^+$ is composed of phenyl and methyl groups. Hence, the spin density on the side chain can be further divided to two parts, phenyl and methyl groups. The spin densities for two parts are plotted in Fig. 2b as a function of n. For $n = 2$, the spin densities on the phenyl and methyl groups are calculated to be 0.41 and −0.01, respectively, indicating that almost all spin densities are distributed on the phenyl group. The spin density on the phenyl group decreases slightly with increasing n. This is due to the fact that the distribution of hole is gradually concentrated to the main chain in the longer chain lengths. For $n = 8$, the spin density on the phenyl group is 0.28.

The hyperfine coupling constants on the hydrogen atoms of the oligosilanes and its average values on phenyl and methyl groups $\langle a_H \rangle$ are given in Table 3. For $n = 2$, the values of $\langle a_H \rangle$ on phenyl and methyl groups are calculated to be 6.08 and 8.46 G, respectively. These values decrease significantly with increasing n. For $n = 8$, $\langle a_H \rangle$'s are 1.77 G for the phenyl group and 3.60 G for the methyl group. For example, the oligosilane with $n = 8$ has 66 hydrogen atoms, predicting that electron spin resonance (ESR) spectrum of $n = 8$ shows a broad band. Actually, ESR spectrum of radical cation of poly(methylphenylsilane) shows a broad spectrum without a fine structure [23]. The present calculation suggests that the broad spectrum of $OMPSi^+$ is originated from multiplication of the hydrogen atoms in polysilane.

3.3. Excitation energies of neutral and radical cation of OMPSi ($n = 4$–8)

The excitation energies of neutral OMPSi are calculated by means of the TDDFT(B3LYP) method with the 3-21G(d) basis set. The results are given in Fig. 3 as simulated absorption spectra. The half-width is assumed to 0.01 eV. The first excitation energies of neutral OMPSi for $n = 4$, 6 and 8 are calculated to be 4.68, 4.49, and 4.25 eV, respectively. The oscillator strength increases with increasing n. This band is assigned to a σ(Si–Si) → σ*(Si–Si) transition of the Si main chain. The second band includes π-character of phenyl group.

The simulated absorption spectra of radical cation $OMPSi^+$ are also illustrated in Fig. 3. The first excitation energies for $n = 4$, 5, 6, 7 and 8 are calculated to be 1.23, 1.18, 1.08, 0.99 and 0.97 eV, respectively, indicating that the first excitation energy of $OMPSi^+$ decreases with increasing n, and it is saturated around $n = 8$. The first excitation energies of $OMPSi^+$ are significantly lower than those of neutral OMPSi. The oscillator strength is gradually increases with increasing n, as well as that of neutral OMPSi. The corresponding experimental excitation energies for $n = 4$, 5, and 6 are measured to be 1.80, 1.70 and 1.60 eV, respectively, indicating that the TDDFT(B3LYP)/3-21G(d) level represents reasonably the excitation energies of $OMPSi^+$. The first excitation energy of radical cation of poly(methylphenylsilane) is measured to be 1.0 eV [24], which is significantly close to the present calculated value (0.97 eV for the saturated excitation energy).

To elucidate the electronic states of $OMPSi^+$ at the first excited state, the coefficients of configuration state function (CSF) are analyzed. The coefficients of CSF contributing to the energy lowering are given in Table 4. The TD-DFT calculation shows that the wave function for the first excited state is approximately expressed by

Table 3
Hyperfine coupling constants (a_H in gauss) of hydrogen atoms in the radical cations of oligo[methyl(phenyl)silane]s (OMPSi$^+$) calculated at the B3LYP/6-311+G(d,p)//B3LYP/3-21G(d) level

n	Ph(1)	Ph(2)	Ph(3)	Ph(4)	Ph(5)	Ph(6)	Ph(7)	$\langle a_H \rangle$
2	6.083	6.083						6.08
3	3.287	5.839	2.608					3.91
4	1.698	3.313	3.911	2.060				2.74
5	1.567	2.966	2.801	2.323	1.050			2.14
6	1.146	2.407	2.346	2.240	1.714	0.762		1.77
n	Me(1)	Me(2)	Me(3)	Me(4)	Me(5)	Me(6)	Me(7)	$\langle a_H \rangle$
2	8.456	8.459						8.46
3	3.367	8.193	5.179					5.58
4	3.741	7.301	6.212	2.116				4.84
5	1.504	4.338	6.228	5.886	2.745			4.14
6	1.119	3.168	4.891	5.655	4.751	2.035		3.60

Averaged values are also given in parenthesis ($\langle a_H \rangle$ in gauss).

$$\psi = C_1\phi(\mathrm{HOMO}-1 \rightarrow \mathrm{HOMO}) + C_2\phi(\mathrm{HOMO} \rightarrow \mathrm{HOMO}+m) + \ldots (\text{where } m > 1)$$

For $n = 8$, the coefficients C_1 and C_2 are calculated to be 0.875 and 0.064, respectively, indicating that the main configuration for the first excited state is ϕ(HOMO $-1 \rightarrow$ HOMO). The orbital for HOMO -1 is mainly composed of π-character of phenyl group. Hence, the first transition of OMPSi$^+$ is assigned to an electronic transition from the phenyl group to the Si main chain.

3.4. Electronic states of dication of OMPSi

For comparison, the excitation energies of dication of OMPSi (denoted by OMPSi^{2+}) are calculated with the same manner. The structures of OMPSi^{2+} are fully optimized at the B3LYP/3-21G(d) level. The optimized geometrical parameters are summarized in Table 5. All Si–Si bonds in OMPSi^{2+} are largely elongated because σ-electrons in bonding orbitals are removed by the dication formation. The elongation is longer than those of cation.

The simulated absorption spectra of OMPSi^{2+} are illustrated in Fig. 3. The first excitation energies of OMPSi^{2+} for $n = 6$, 7 and 8 are calculated to be 1.35, 1.25, and 1.23 eV, respectively. The first excitation bands are slightly blue-shifted from those of OMPSi$^+$, while the intensities for the electronic transition of dication are larger than those of radical cation.

4. Discussion

4.1. Summary

In the present study, the DFT calculations were applied to the radical cations of oligo[methyl(phenyl)silane] OMPSi$^+$ ($n = 2$–8) to elucidate the electronic states. The unpaired electron (hole) are distributed in both main and side chains, although the spin density in the main chain is lager than that of side-chain (70% in the Si-main chain and 30% in the side-chain). These features are much different from that of radical cation of oligo(dimethyl)silane ODMSi$^+$: almost all hole is localized in the Si-main chain.

4.2. Comparison with previous studies

Previous experiments showed that the introduce of aromatic group into the side chain of polysilane enhances strongly the hole conductivity. Seki et al. speculate that the interchain hole transfer takes place via phenyl groups [16]. The present study supports strongly their speculation. Namely, the present calculation indicates that the substitution of the methyl group to the phenyl group increases significantly the spin density on the side chain. This causes the

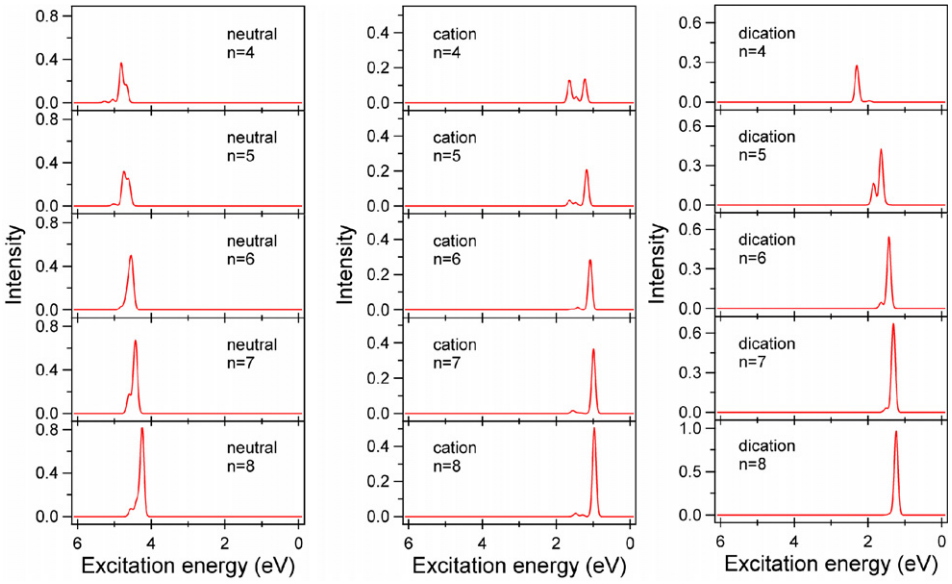

Fig. 3. Simulated absorption spectra of neutral, cation and dication of OMPSi calculated at the B3LYP/3-21G(d) level. The half-width is assumed to be 0.01 eV. It is assumed that each peak is distributed by Gaussian shape.

Table 4
Coefficients of configuration state functions (C_1 and C_2), excitation energies (E_{ex} in eV), and oscillator strengths (f) of $OMPSi^+$ calculated by TD-DFT(B3LYP)/3-21G(d) method

State	n	E_{ex} (eV)	f	C_1	Configuration[a]	C_2	Configuration
Neutral	1	5.50	0.0026	0.540	32 → 34	−0.473	33 → 35
	2	5.24	0.5320	0.660	65 → 66	0.095	61 → 66
	3	4.89	0.2113	0.664	97 → 98	−0.166	97 → 99
	4	4.68	0.1601	0.629	129 → 130	−0.276	129 → 131
	5	4.58	0.0851	0.659	161 → 162	−0.175	161 → 164
	6	4.49	0.0858	0.615	193 → 194	−0.260	193 → 196
	7	4.40	0.1551	0.647	225 → 226	−0.226	225 → 228
	8	4.25	0.8054	0.656	257 → 258	0.173	257 → 259
Cation	2	1.32	0.0005	0.999	62B → 65B	−0.099	64B → 65B
	3	1.16	0.0007	0.997	95B → 97B	−0.092	94B → 97B
	4	1.23	0.1361	0.919	128B → 129B	0.056	127B → 129B
	5	1.18	0.2080	0.914	160B → 161B	−0.044	161A → 165A
	6	1.08	0.2838	0.898	192B → 193B	−0.054	193A → 198A
	7	0.99	0.3676	0.880	224B → 225B	0.063	225A → 231A
	8	0.97	0.5070	0.875	256B → 257B	0.064	257A → 261A

[a] Orbital numbers of HOMO for $n = 1$–8 of OMPSi are 32 ($n = 1$), 65 ($n = 2$), 97 ($n = 3$), 129 ($n = 4$), 161 ($n = 5$), 193 ($n = 6$), 225 ($n = 7$), and 257 ($n = 8$), respectively.

Table 5
Optimized geometrical parameters of Si–Si bond lengths (in Å) and dihedral angles of dication of oligo[methyl(phenyl)silane]s ($OMPSi^{2+}$) calculated at the B3LYP/3-21G(d)

	n	Si(n) to Si($n+1$) length (Å)						
		Si(1–2)	Si(2–3)	Si(3–4)	Si(4–5)	Si(5–6)	Si(6–7)	Si(7–8)
Dication	4	2.4606	2.4629	2.4605				
	5	2.4462	2.4331	2.4058	2.4738			
	6	2.4409	2.4165	2.4218	2.4154	2.4488		
	7	2.4225	2.4052	2.4145	2.4234	2.4053	2.4249	
	8	2.4159	2.4094	2.4086	2.4295	2.4088	2.4046	2.4145
State	n	Dihedral angle (°)						
		Si(1–2–3–4)	Si(2–3–4–5)		Si(3–4–5–6)	Si(4–5–6–7)		Si(5–6–7–8)
Dication	4	177.5						
	5	173.9	164.2					
	6	156.0	156.7		156.3			
	7	164.8	164.3		160.8	161.2		
	8	167.5	174.8		158.7	158.3		158.3

increase of hole hopping probability between polymer chains.

Toma et al. investigated $OMPSi^+$ ($n = 10$) using the similar level of theory. They suggested that a positive hole is distributed on 58% in phenyl group and 36% in methyl group. This result is in qualitatively agreement with our results.

Kumagai et al. measured absorption spectra of $OMPSi^+$ ($n = 2$) and polymethylphenylsilane radical cation (poly-$MPSi^+$). The $OMPSi^+$ ($n = 2$) shows a broad band with absorption maximum at 2.06 eV, while poly-$MPSi^+$ has absorption maximum at 1.00 eV. The present calculation indicates that excitation energies of $OMPSi^+$ ($n = 2$) with strong oscillator strengths are 1.87 and 2.18 eV, which are in good agreement with Kumagai's data. Also, the excitation energies of $OMPSi^+$ ($n = 8$) is calculated to be 1.0 eV, which is agreed well with the experiments. This agreement implies that the level of theory is enough to discuss the electronic states of $OMPSi^+$.

4.3. Model of hole transport in $OMPSi^+$

In this section, mechanism of hole-transport in the radical cation of oligosilanes is discussed on the basis of theoretical results. Model of hole-transfer process in $ODMSi^+$ (upper) and $OMPSi^+$ (lower) derived from the present calculation is schematically illustrated in Fig. 4. In the case of radical cation of ODMSi, spin density is fully localized in the Si main chain, while the spin density on the side chain (methyl group) is negligibly small. Therefore, the hole can be transferred along the main chain. The intermolecular hole-transfer is hardly occurred at the ground state in $ODMSi^+$.

On the other hand, in the case of $OMPSi^+$, the spin density is widely distributed on both main and side chains, suggesting that the intermolecular hole transfer easily takes place via the phenyl groups of $OMPSi^+$. Thus, the hole transport mechanisms in both polymers are essentially different each other.

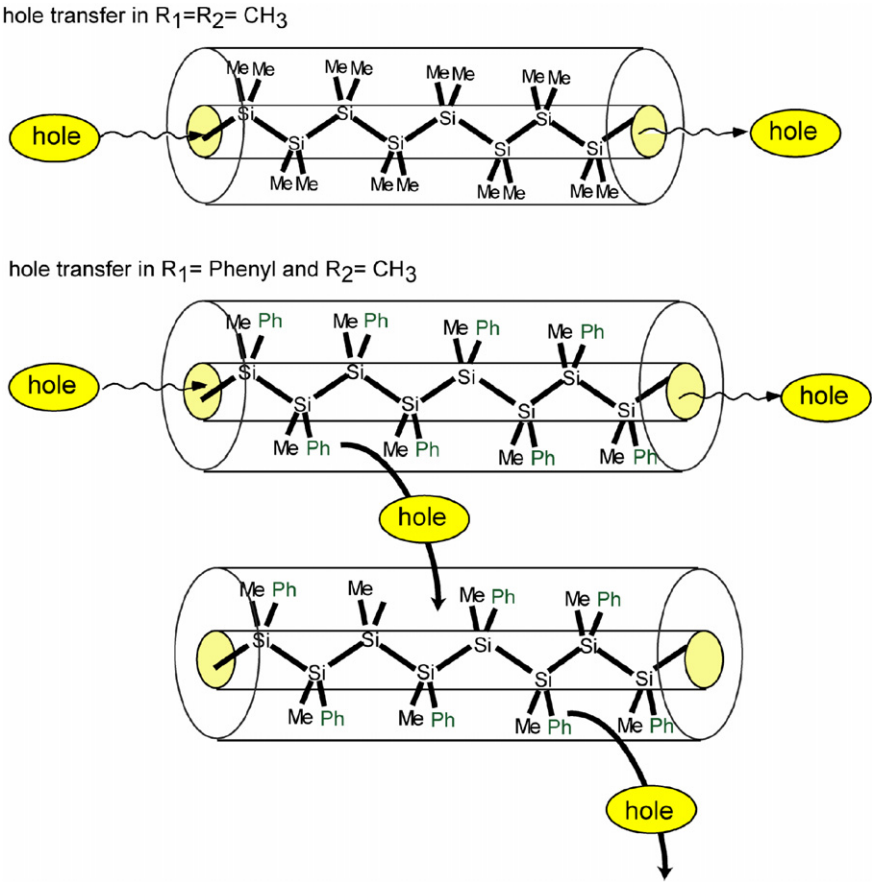

Fig. 4. Models of hole transport in radical cations of oligo(dimethyl)silane ODMSi (upper) and that of oligo[methyl(phenyl)silane] OMPSi (lower).

Acknowledgements

The authors are indebted to the Computer Center at the Institute for Molecular Science (IMS) for the use of the computing facilities. Also, the author (H.K.) acknowledges a partial support from President's optional budget from Kyoto University. One of the authors (H.T.) acknowledges a partial support from a Grant-in-Aid for Scientific Research (C) from the Japan Society for the Promotion of Science (JSPS).

References

[1] R.D. Miller, J. Michl, Chem. Rev. 89 (1989) 1359.
[2] S. Nespurek, J. Sworakowski, A. Kadashchuk, P. Toman, J. Organometal. Chem. 685 (2003) 269.
[3] F.K. Perkins, E.A. Dobisz, S.L. Brandow, J.M. Calvert, J.E. Kosakowski, C.R.K. Marrian, Appl. Phys. Lett. 68 (1996) 550.
[4] H. Suzuki, S. Hoshino, C.H. Yuan, M. Fujiki, S. Toyoda, N. Matsumoto, IEEE J. Quantum Electron. 4 (1998) 129.
[5] R. Hattori, T. Sugano, J. Shirafuji, T. Fujiki, Jpn. J. Appl. Phys. 35 (1996) L1509.
[6] Y. Xu, T. Fujino, S. Watase, H. Naito, K. Oka, T.. Dohmaru, Jpn. J. Appl. Phys. 38 (1999) 2609.
[7] H. Suzuki, S. Hoshino, C.H. Yuan, M. Fujiki, S. Toyoda, N. Matsumoto, Thin Solid Films 331 (1998) 64.
[8] K. Okamoto, T. Tojo, H. Tada, M. Terazima, K. Matsushige, Mol. Cryst. Liq. Cryst. 370 (2001) 379.
[9] H. Suzuki, S. Hoshino, K. Furukawa, K. Ebata, C.H. Yuan, I. Bleyl, Polym. Adv. Technol. 11 (2000) 460.
[10] M. Hiramoto, Y. Sakata, M. Yokoyama, Jpn. J. Appl. Phys. 35 (1996) 4809.
[11] R.G. Kepler, J.M. Zeigler, L.A. Harrah, S.R. Kurtz, Phys. Rev. B 35 (1987) 2818.
[12] M.A. Abkowitz, M.J. Rice, M. Stolka, Phil. Mag. 61 (1990) 25.
[13] G.P. Van de Laan, M.P. De Haas, J.M. Marman, H. Frey, Möller, M. Mol. Cryst. Liq. Cryst. 236 (1993) 165.
[14] H. Frey, M. Möller, M.P. De Haas, N.J.P. Zenden, P.G. Schouten, G.P. Van de Laan, M.P. De Haas, J.M. Marman, Macromolecules 26 (1993) 89.
[15] G.P. Van de Laan, M.P. De Haas, A. Hummel, H. Frey, S. Scheiko, M. Möller, Macromolecules 27 (1994) 1897.
[16] S. Seki, Y. Koizumi, T. Kawaguchi, H. Habara, S. Tagawa, J. Am. Chem. Soc. 126 (2004) 3521.
[17] S. Irie, M. Irie, Macromolecules 25 (1992) 1766.
[18] P. Toman, S. Nespurek, J.W. Jang, C.E. Lee, Int. J. Quant. Chem. 101 (2005) 746.
[19] H. Tachikawa, H. Kawabata, J. Organomet. Chem. 691 (2006) 4843.
[20] M.J. Frisch, G.W. Trucks, H.B. Schlegel, G.E. Scuseria, M.A. Robb, J.R. Cheeseman, J.A. Montgomery Jr., T. Vreven, K.N. Kudin, J.C. Burant, J.M. Millam, S.S. Iyengar, J. Tomasi, V. Barone, B. Mennucci, M. Cossi, G. Scalmani, N. Rega, G.A. Petersson, H. Nakatsuji, M. Hada, M. Ehara, K. Toyota, R. Fukuda, J. Hasegawa, M. Ishida, T. Nakajima, Y. Honda, O. Kitao, H. Nakai, M. Klene, X. Li, J.E. Knox, H.P. Hratchian, J.B. Cross, C. Adamo, J. Jaramillo, R. Gomperts, R.E. Stratmann, O. Yazyev, A.J. Austin, R. Cammi, C. Pomelli, J.W. Ochterski, P.Y. Ayala, K. Morokuma, G.A. Voth, P. Salvador, J.J. Dannenberg, V.G. Zakrzewski,

Dapprich, A.D. Daniels, M.C. Strain, O. Farkas, D.K. Malick, A.D. Rabuck, K. Raghavachari, J.B. Foresman, J.V. Ortiz, Q. Cui, A.G. Baboul, S. Clifford, J. Cioslowski, B.B. Stefanov, G. Liu, A. Liashenko, P. Piskorz, I. Komaromi, R.L. Martin, D.J. Fox, T. Keith, M.A. Al-Laham, C.Y. Peng, A. Nanayakkara, M. Challacombe, P.M.W. Gill, B. Johnson, W. Chen, M.W. Wong, Gonzalez, J.A. Pople, GAUSSIAN 03, Revision B.04, Gaussian, Inc., Pittsburgh PA, 2003.

[21] H. Tachikawa, H. Kawabata, J. Mater. Chem. 13 (2003) 1293.

[22] H. Tachikawa, H. Kawabata, J. Phys. Chem. B 107 (2003) 1113.

[23] H. Tachikawa, H. Kawabata, J. Phys. Chem. B 109 (2005) 3139.

[24] J. Kumagai, H. Yoshida, T. Ichikawa, J. Phys. Chem. 99 (1995) 7965.